

# Stereoscopic electron spectroscopy of solar hard X-ray flares with a single spacecraft

Eduard P. Kontar and John C. Brown

*Department of Physics and Astronomy, The University of Glasgow, G12 8QQ, UK*

eduard,john@astro.gla.ac.uk

## ABSTRACT

Hard X-ray (HXR) spectroscopy is the most direct method of diagnosing energetic electrons in solar flares. Here we present a technique which allows us to use a single HXR spectrum to determine an effectively stereoscopic electron energy distribution. Considering the Sun's surface to act as a 'Compton mirror' allows us to look at emitting electrons also from behind the source, providing vital information on downward-propagating particles. Using this technique we determine simultaneously the electron spectra of downward and upward directed electrons for two solar flares observed by the Ramaty High Energy Solar Spectroscopic Imager (RHESSI). The results reveal surprisingly near-isotropic electron distributions, which contrast strongly with the expectations from the standard model which invokes strong downward beaming, including collisional thick-target model.

*Subject headings:* Sun: flares — Sun: particle emission — Sun: X-rays, gamma rays

## 1. Introduction

Energetic electrons and ions have long been considered (Ellison and Hoyle, 1947) as possibly playing a key role in energy release by magnetic reconnection, in phenomena such as solar flares (Aschwanden, 2002), which are archetypes of magnetic explosions and particle acceleration in the cosmos, as well as being central to space weather and its terrestrial influence.

The spectrum of energetic electrons and the anisotropy of source electrons are normally inferred separately. Hard X-ray (HXR) directivity itself has, until now, been measured using two different techniques. The first is direct simultaneous measurement of flux spectra from at least two spacecraft at well separated locations (Li et al, 1994; Kane et al 1988). The second method is based on the statistical study of the distribution of HXR fluxes and spectral indices over heliocentric angle (Datlowe et al. 1977; Bogovalov et al. 1985; Vestrland 1987). However, neither of these methods provides direct information about downward emitted photons which are crucial in model

testing.

High resolution HXR spectrometry with RHESSI enables reconstruction of volume-averaged source electron flux spectra ( $\text{electrons cm}^{-2} \text{s}^{-1} \text{keV}^{-1}$ ) from bremsstrahlung HXR emission spectra (photons  $\text{electrons cm}^{-2} \text{s}^{-1} \text{keV}^{-1}$ ) observed at the Earth (Piana et al. 2003; Kontar et al. 2004). However, the observed spectrum is contaminated by an albedo component, due to Compton back-scattering ('reflectivity') in the dense photosphere, of those primary bremsstrahlung photons which were emitted downward (Tomblin, 1972; Bai and Ramaty, 1978). Until now this albedo contribution has been regarded as a nuisance to be corrected for, either following Bai and Ramaty (Johns and Lin 1992, Alexander and Brown 2002;), or self-consistently (Kontar et al, 2006), before spectral inference of electron spectra.

In this Letter we show that, on the contrary, the albedo spectral 'contaminant' in fact offers very valuable insight into the anisotropy of the flare fast electron distribution. It does so by providing a view of the HXR flare from behind, like a dentist's mirror, except that the solar albedo mir-

ror is spectrally distorting so its contribution to the overall spectrum can be distinguished. This reflectivity has a broad spectral peak in the 30-50 keV range (Bai and Ramaty, 1978; Kontar et al, 2006). It decreases fast at low energies due to photoelectric absorption while high energy photons are more likely to be lost to an observer because they penetrate too deep into the solar atmosphere to be scattered back to an external observer. On the other hand, an important property of bremsstrahlung emission is that it is always monotonically decreasing for any electron spectrum, typically having a roughly power-law shape of spectral index which is nowhere less than 1 (Koch and Motz, 1959). Thus, the primary emission and the albedo 'bump' spectral signatures are very distinct. The observed spectrum in the observer's direction should contain an albedo bump feature, the strength of which is an indicator of the degree of downward beaming of the electron distribution. By use of this solar 'mirror' we can achieve a degree of 2-directional beam electron beam spectrometry from single spacecraft photon spectrometry.

We show furthermore that this insight constrains the directivity of flare electrons, so strongly that the conventional solar flare models with downward beaming are excluded. Note that the inferred electron spectra and distributions cannot be explained by the collisional scattering (Trubnikov 1965) as assumed in collisional thick-target (CTT) model (e.g. Brown 1971; Brown 1972). In the CTT scenario, even allowing for collisional scattering, the downward-propagating electrons emit HXR bremsstrahlung which is also substantially downward-collimated.

## 2. Photospheric albedo as a natural constraint on downward beaming of electrons

For an inhomogeneous bremsstrahlung source of volume  $V$ , plasma density  $n(\mathbf{r})$ , and electron flux spectrum  $F(E, \mathbf{\Omega}', \mathbf{r})$  per unit solid angle in direction  $\mathbf{\Omega}'$  can be averaged over the source volume. The photon flux spectrum at Earth distance  $R$  in direction  $\mathbf{\Omega}$  is

$$I(\epsilon) = \frac{\bar{n}V}{4\pi R^2} \int_{\mathbf{\Omega}'} \int_{\epsilon}^{\infty} \bar{F}(E, \mathbf{\Omega}') Q(\mathbf{\Omega}, \mathbf{\Omega}', \epsilon, E) dE d\mathbf{\Omega}' \quad (1)$$

where  $Q(\mathbf{\Omega}, \mathbf{\Omega}', \epsilon, E)$  is the bremsstrahlung cross section differential in  $\epsilon$  and  $\mathbf{\Omega}$ ;  $\bar{n} = V^{-1} \int n(\mathbf{r}) dV$  is a volume averaged density, the density-weighted mean electron flux is  $\bar{F}(E, \mathbf{\Omega}') = (\bar{n}V)^{-1} \int n(\mathbf{r}) F(E, \mathbf{\Omega}', \mathbf{r}) dV$ , and  $\epsilon$ , and  $E$  are photon and electron energies correspondingly. In fact  $Q$  depends only on the angle  $\mathbf{\Omega}'\mathbf{\Omega}$  between the incoming electron  $\mathbf{\Omega}'$  and the emitted photon  $\mathbf{\Omega}$  directions.

Equation (1) can be approximated using a two directional representation based on the fact that here we are concerned with emission upward ( $u$ ) toward the observer and downward ( $d$ ) toward the scattering photosphere. The flux toward the observer  $I_o(\epsilon, \theta)$  from a source with heliocentric angle  $\theta$  can be written

$$I_o(\epsilon) = \frac{1}{4\pi R^2} \bar{n}V \int_{\epsilon}^{\infty} [Q^F(\epsilon, E) \bar{F}_u(E) + Q^B(\epsilon, E) \bar{F}_d(E)] dE, \quad (2)$$

where  $\bar{F}_{u,d} = (\bar{n}V)^{-1} \int F_{u,d}(E, \mathbf{r}) n(\mathbf{r}) dV$  and, using axial symmetry, we have introduced

$$Q(\epsilon, E, \theta_0) = \frac{1}{\cos(\theta_0 - \Delta\theta) - \cos(\theta_0 + \Delta\theta)} \int_{\theta_0 - \Delta\theta}^{\theta_0 + \Delta\theta} Q(\epsilon, E, \theta') \sin(\theta') d\theta' \quad (3)$$

the cross-section averaged over  $[\theta_0 - \Delta\theta, \theta_0 + \Delta\theta]$  and centered at angle  $\theta_0$ . Hence,  $Q^F(\epsilon, E) \equiv Q(\epsilon, E, \theta_0 = 0)$  and  $Q^B(\epsilon, E) \equiv Q(\epsilon, E, \theta_0 = 180^\circ - \theta)$ , where  $\theta$  is the heliocentric angle of the source. Electron spectrum  $\bar{F}(E, \theta)$  is defined in a similar two directional approximation:  $\bar{F}_u(E)$  and  $\bar{F}_d(E)$  are the density weighted volumetric mean flux spectra of electrons directed towards the observer 'upward' and downward respectively, also averaged over  $\Delta\theta$ .

The probability of photon emission along the direction of motion is around ten times higher than in the opposite direction and four times that at right angle, the cross-section having a typical angular scale  $\Delta\theta \sim 30 - 50^\circ$  (Koch and Motz, 1959) for energies 50-300 keV. Moreover, the electron distribution should have some additional angular spread (e.g. because of collisions (Trubnikov, 1965; Brown 1972, Leach and Petrosian 1983, MacKinnon and Craig, 1992) and magnetic field convergence). Therefore, for the spatially averaged distribution it is natural to deal with angular distribution averaged over  $\Delta\theta$ . In our

calculations we take  $\Delta\theta = 45^\circ$  as a characteristic scale of angular dependency. (In the limit  $\Delta\theta = 180^\circ$  the cross-section becomes angle averaged and equation (2) is reduced to the simplified equation for isotropic electron distributions used in, e.g., Brown et al., (2003)).

X-ray photons propagating downwards undergo Compton backscattering and absorption in the dense photosphere, the spatially integrated reflected flux being expressible via a Green's function approach (Magdziarz and Zdziarski, 1995; Kontar et al, 2006).

$$I_r(\epsilon) = \int_{\epsilon}^{\infty} G(\mu, \epsilon, \epsilon') I_d(\epsilon') d\epsilon' \quad (4)$$

where  $I_d(\epsilon)$  is the the downward directed flux and  $G(\mu, \epsilon, \epsilon')$  is the angular ( $\mu = \cos(\theta)$ ) dependent Green's functions (Kontar et al, 2006). The reflected flux can be written

$$I_r(\epsilon, \mu) = \frac{\bar{n}V}{4\pi R^2} \int_{\epsilon}^{\infty} G(\mu, \epsilon, \epsilon') d\epsilon' \int_{\epsilon'}^{\infty} [Q^F(\epsilon', E) \bar{F}_d(E) + Q^B(\epsilon', E) \bar{F}_u(E)] dE, \quad (5)$$

where we use the same cross-sections as in Equation (3).

The total observed flux is the sum of direct and back-scattered X-rays, i.e.,  $I(\epsilon) = I_o(\epsilon) + I_r(\epsilon)$  with  $I_o(\epsilon)$ ,  $I_r(\epsilon)$ , given by Equations (2), (5). Even using a single spacecraft we thus always observe a combination of reflected downward flux and direct flux which are functionally very different. This fact, and the properties of bremsstrahlung emission, allow us to draw, from spectral data, conclusions about both the directivity and the spectrum of the emitting electron distribution.

Figure (1) shows that albedo sets a natural constraint on possible directivity present in solar flares. Strong downward directivity (all electrons are confined within a pitch angle of  $45^\circ$ ) typical to the collisional models (e.g. Brown, 1972; MacKinnon and Craig, 1992) leads to flatter than observed spectral indices below 20 keV and softer than observed spectra in the hundreds of keV range. It can be seen that the observed spectral index at 200-300 keV cannot be less than 5 (Figure (1), much softer than typical spectral indices 2–3 (Vestrand et al, 1987; Li et al, 1994).

### 3. Two directional electron distributions

In reality we deal with discrete data sets rather than continuous functions. Therefore, the data vector of photons  $\mathbf{I}(\epsilon_i) = \mathbf{I}_o + \mathbf{I}_r$  can be written

$$\mathbf{I} = \begin{pmatrix} \mathbf{Q}^F + \mathbf{G}(\mu)\mathbf{Q}^B & \mathbf{Q}^B + \mathbf{G}(\mu)\mathbf{Q}^F \end{pmatrix} \begin{pmatrix} \bar{\mathbf{F}}_d \\ \bar{\mathbf{F}}_u \end{pmatrix} \quad (6)$$

where  $\epsilon_i$  for  $i = 1...N$ , and  $E_j$  for  $j = 1...M$ , where  $\bar{\mathbf{F}}_{d,u}(E_j)$  are the electron data vectors and  $\mathbf{G}$ ,  $\mathbf{Q}^{B,F}$  are matrix representations of the kernels of integral equations (2,5). Green's matrixes  $\mathbf{G}(\mu)$  depend on heliocentric angle of the source  $\mu = \cos(\theta)$  and have been calculated in Kontar et al., 2006. The multiple sum in Equation (6)  $\Sigma^M \Sigma^2$  can be expressed as a single sum  $\Sigma^{2M}$  (Hubeny and Judge 1995). Equation (6) can be solved using the Tikhonov (1963) regularization method of which our implementation was successfully tested by simulation (Kontar et al. 2004) and applied to RHESSI data (Kontar et al. 2005).

To test our method we applied it to simulated data from known electron distributions, adding typical noise. Two different forms of anisotropy: 'weak' anisotropy  $\bar{F}_u(E) = \bar{F}_d(E)/(1 + \sqrt{(E-10)/50})$  and 'strong' anisotropy  $\bar{F}_u(E) = \bar{F}_d(E)/(1 + \sqrt{(E-10)/50})^2$  in downward direction. From the simulated photon spectra we inferred regularized electron fluxes ( $\bar{F}_u(E), \bar{F}_d(E)$ ). The results demonstrate that the method used recovers reliably the directional electron spectra. However, the method is not sensitive to too 'weak' anisotropy that gives us anisotropy sensitivity. The difference between  $\bar{F}_u(E)$  and  $\bar{F}_d(E)$  for the case of 'weak' anisotropy is within the error bars.

First we consider some limiting cases.

**If all electrons were purely downward directed** (e.g.  $\bar{F}_d \neq 0$   $\bar{F}_u = 0$  in Equation (6)) then the observed spectrum would be mostly given by reflected and backward emitted photons (Figure 2). Since the efficiency of Compton scattering as well as the efficiency of backward emission ( $Q_B(E, \epsilon) \ll Q_F(E, \epsilon)$  for  $E, \epsilon > 50$  keV) decrease fast with energy, the photon spectrum should be rather steep. The photon spectral index should be not less than 5 (Figure 1) in the 200-300 keV energy range even for a flat power-law electron spectrum while the typical spectral index observed is around three (Aschwanden, 2002). Moreover, the inverse approach concludes that for the Au-

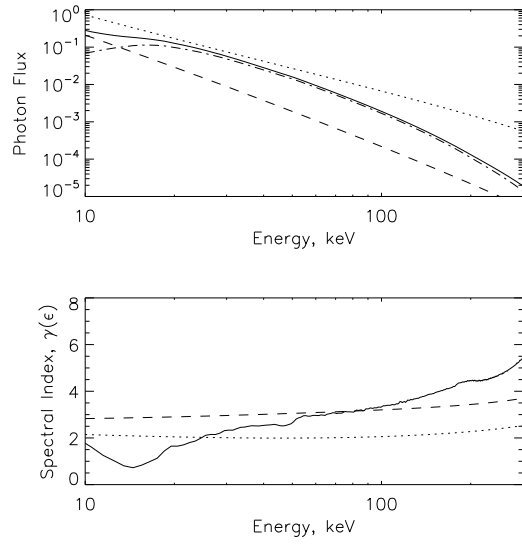


Fig. 1.— Simulated photon flux spectra (upper panel) and spectral index (lower panel) for a flare located at heliocentric angle  $\theta = 40^\circ$  with electron distribution ( $\bar{F}_d(E) \sim E^{-1.5}$  and  $\bar{F}_u(E) = 0$ , e.g., all electrons are directed downward and confined within pitch angle of  $\pm 45^\circ$ ). Upper panel: Observed (solid line), downward directed (dotted line), upward directed (dash line) and reflected (dash-dotted line) flux spectra. Lower panel: observed (solid), upward (dotted), and downward (dashed) spectral indexes.

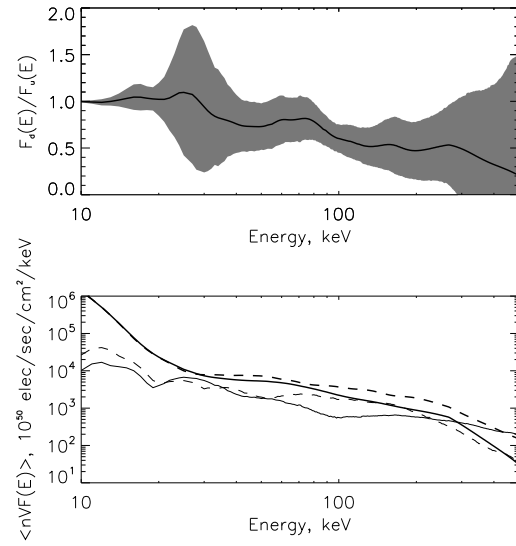


Fig. 2.— Lower panel: The recovered mean electron flux spectra (thick lines) for August 20, 2002 flare (accumulation time interval 08:25:20-08:25:40 UT) downward-directed  $\bar{F}_d(E)$  (solid line) and observer-directed  $\bar{F}_u(E)$  (dash line) with corresponding errors (thin lines). Upper panel: electron anisotropy defined as  $\bar{F}_d(E)/\bar{F}_u(E)$  with confidence values within shaded area.

gust 20, 2002 flare (Kasparova et al, 2005), if the HXRs were strongly downward beamed (within a pitch angle of  $45^\circ$ ) the electron spectrum required would have to grow above 400 keV to fit the data which casts doubt on the original assumption of downward beaming.

**If we ignore albedo** Equation (6) leads to a substantial gap or low energy cutoff in the mean electron spectrum (e.g. Kasparova et al, 2005), hence the local speed distribution function  $f(v) = \bar{F}(E)dE/dv/v$  has a positive derivative. Such distributions are unstable and relax in the solar corona on a timescale much shorter than our observing time interval (e.g., Emslie and Smith 1984, Melnik et al, 1999).

We now consider the spectra at the peak of two solar flares: August 20, 2002 around 08 : 20 UT (heliocentric angle  $\sim 40^\circ$ ) and January 17, 2005 around 09 : 40 UT (heliocentric angle  $\sim 33^\circ$ ). Both have sufficiently high count rates for good statistics up to above 500 keV but not so high as to cause severe pulse pile-up effects (Smith et al, 2002). We used 7 out of 9 front RHESSI segments, excluding detectors 2 and 7 due to their low energy resolution at the time of observation (Smith et al, 2002). Naturally we have chosen events not far from the disk centre since limb events are not suitable for our analysis because albedo is almost negligible for such flares.

The general properties of the August 20, 2002 flare  $\sim 08 : 20$ UT, which matched our count rate criteria, were extensively analyzed in Kasparova et al, 2005. To fit the hard X-ray spectrum with a double power-law electron spectrum with a low energy cut-off  $E_c$  and ignoring albedo, requires an unusually high value of  $E_c \sim 30 \pm 2$  keV. This produces a clear gap in the overall  $\bar{F}(E)$  in the range 15-30 keV which is likely to be unphysical and suggests albedo is important.

Figure 2 shows electron spectra solutions ( $\bar{F}_d(E), \bar{F}_u(E)$ ) with the confidence strips of our inferred downward and upward electron flux spectra. The results are close to consistent with isotropy up to 100 keV with some indication of upward anisotropy above 100 keV. Purely isotropic distribution would be given by unity, e.g.  $\bar{F}_u(E) = \bar{F}_d(E)$ . The January 17, 2004 flare has similar characteristics (Figure 3): a rather flat spectrum (photon spectral index  $\leq 2.3$ ) and good count rate up to a few hundred keV. However,

this flare started in the soft X-ray tail of another event. To avoid difficulties with background subtraction, we used data only from 15 keV.

#### 4. Discussions and conclusions

The analysis of RHESSI spectra shows that we can infer simultaneously information on the directional and the energy distributions of electrons. It is clear that for the January 17 flare (Figure 3) that the  $\bar{F}_d(E), \bar{F}_u(E)$  solution are so overlapping and ratio  $\bar{F}_d(E)/\bar{F}_u(E)$  is so close to unity that the electron distribution is consistent with isotropy at all  $E$ . For the August 20 flare in Figure 2, the distribution is consistent with isotropy at low  $E$  (below 100 keV) but may be slightly beamed toward the observer at high  $E$ . Since our recoveries are means about just 2 directions, a wide range of actual  $\mu$  distributions are consistent with them. For example, the August 20 event somewhat resembles a 'pancake' distribution of particles circling perpendicular to the magnetic field, so that perpendicular component of electron energy should be slightly larger than parallel one (Figure 2). However, none of these results resembles the beam-like form expected for the basic CTT model. For example, a simplified mean particle treatment (Brown, 1972) has no electrons propagating upward, while more detailed dispersive treatments (MacKinnon and Craig 1991) suggests downward anisotropies of up to  $\bar{F}_d(E)/\bar{F}_u(E) \sim 10 - 100$  depending on energy and on initial pitch angle distribution. Full Fokker-Planck models including magnetic mirroring with a converging magnetic field (Leach and Petrosian 1981) give larger upward flux but still predominantly downward and outside our confidence interval. For the large fluxes involved, these events may involve substantial return current  $E$ -fields which can produce some upward 'beaming' but the effect is larger at lower below 70-75 keV, not higher, energies (Zharkova and Gordovskyy 2005). More advanced self-consistent models with collective effects included are needed for detailed comparisons with the observations.

In conclusion, when allowance is made for the albedo contribution to the observed HXR spectra, the absence of a strong albedo feature precludes the basic model with strong downward beaming including CTT models, at least for the two intense hard solar disk events we have analyzed. This

casts serious doubt on the CTT model, at least in terms of the usually adopted geometry and on its physical basis. Alternatives to the CTT Standard Model may need to be considered, in which acceleration occurs in such a way that collimated injection into a cold target is not involved. For example, HXR source electrons could be locally and continuously reaccelerated with near isotropy along the entire length of a magnetic loop. This model may also solve some of the other difficulties associated with the CTT model such as the problematic high beam density involved.

We gratefully acknowledge the support of a PPARC Advanced Fellowship (EPK) and a PPARC Rolling Grant (JCB). We also note support of ISSI, Bern, Switzerland. We are thankful to Lyndsay Fletcher, Joe Khan, Alec MacKinnon and Säm Krucker for comments and discussions.

## REFERENCES

- Alexander R.C. and Brown J.C., 2002, *Solar Physics*, **210**, 407.
- Aschwanden, M. J., 2002, *Space Sci. Rev.*, **101**, 1.
- Bai, T. and Ramaty, R., 1978, *ApJ*, **219**, 705.
- Bogovalov, S. V., et al, 1985, *Sov. Astronomy Letters*, **11**, 322.
- Brown, J.C., 1971, *Solar Phys.*, **18**, 489.
- Brown, J.C., 1972, *Solar Phys.*, **26**, 441.
- Brown, J.C., et al., 2003, *ApJ*, **595**, L115.
- Datlowe, D. W., et al., 1977, *ApJ*, **212**, 561.
- Ellison, M.A. and Hoyle, F., 1947, *The Observatory*, **67**, 181.
- Emslie, A.G. and Smith, D.F., 1984, *ApJ*, **279**, 882.
- Hubeny, V. and Judge, P.G., 1995, *ApJ*, **448**, L61.
- Johns, C., and Lin, R.P., 1992, *Solar Phys.*, **137**, 121.
- Kane, S. R., et al., 1988, *ApJ*, **326**, 1017.
- Kasparova, J., et al, 2005, *Solar Phys.*, **232**, 63.
- Koch, H. W. and Motz, J. W., 1959, *Phys. Rev.*, **31**, 920.
- Kontar, E.P., et al., 2004, *Solar Phys.*, **225**, 293.
- Kontar, E.P., et al., 2005, *Solar Phys.*, **226**, 317.
- Kontar, E.P., et al., 2006, *Astron. & Astrophys.*, **446**, 1157.
- Leach, J. and Petrosian, V., 1981, *ApJ*, **251**, 781.
- Li, P., et al., 1994, *ApJ*, **426**, 758.
- Lin, R.P. et al., 2002, *Solar Phys.*, **210**, 3.
- Lin, R. P., 1985, *Solar Phys.*, **100**, 537
- MacKinnon, A. L. and Craig, I. J. D., 1991, *Astron & Astrophys.*, **251**, 693.
- Mel'nik, V. N. et al, 1999, *Solar Phys.*, **184**, 353.
- Magdziarz, P., & Zdziarski, A. A., 1995, *MNRAS*, **273**, 837.
- Piana et al., 2003, *ApJ* **595**, L127.
- Smith, D.M. et al., 2002, *Solar Physics*, **210**, 33.
- Tikhonov, A. N., 1963, *Soviet Math. Dokl.*, **4**, 1035.
- Tomblin, F.F., 1972, *ApJ*, **171**, 377.
- Trubnikov, B.A., 1965, *Reviews of Plasma Physics*, **1**, 105.
- Vestrand, W.T. et al., 1987, *ApJ*, **322**, 1010.
- Zharkova, V.V. and Gordovskyy, M., 2005, *Astron. & Astrophys.*, **432**, 1033.

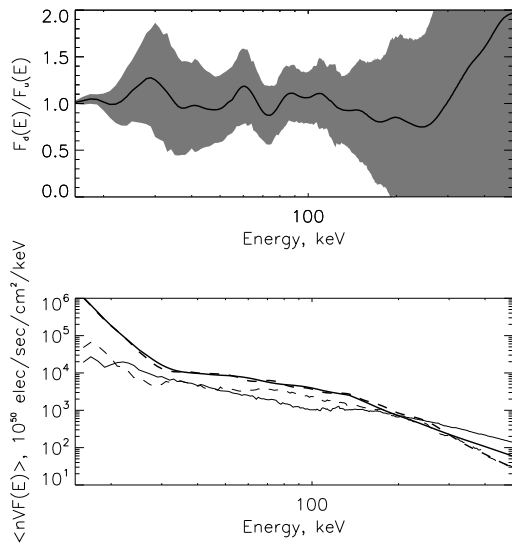


Fig. 3.— The same as Figure (2) but for January 17, 2005 flare (accumulation time interval 09:43:24-09:44:20 UT).